Heat Transfer Performance of Cosine-Shaped Runners

Ping Huang
School of Environment and Safety Engineering, Fuzhou University, Fuzhou, Fujian
Wei Huang
Straits Institute of Minjiang University
Xiajun Lin
School of Environment and Safety Engineering, Fuzhou University, Fuzhou, Fujian
Chi-Min Shu (shucm@yuntech.edu.tw)
National Yunlin University of Science and Technology

Research Article

Keywords: cosine-wave-shaped, structural parameters, synergy angles, CFD software, nonuniformity, shaped channels.

Posted Date: July 22nd, 2021

DOI: https://doi.org/10.21203/rs.3.rs-736850/v1

Heat transfer performance of cosine-shaped runners

Ping Huang[1], Wei Huang[2,3,5], Xiajun Lin[1], Chi-Min Shu[4,6]

[1] School of Environment and Safety Engineering, Fuzhou University, Fuzhou, Fujian

[2]Department of Business Administration, Straits Institute of Minjiang University, Fuzhou, Fujian

[3]Institute of Cross-Strait Higher Education Cooperation and Exchange of Minjiang University, Fuzhou, Fujian, China

[4]Department of Safety, Health, and Environmental Engineering, National Yunlin University of Science and Technology, Yunlin, Taiwan, ROC

[5]Corresponding author at Department of Business Administration, Straits Institute of Minjiang University, Fuzhou, Fujian 350108, China. wei.huang5@mail.mcgill.ca

[6]Corresponding author at Department of Safety, Health, and Environmental Engineering, National Yunlin University of Science and Technology, Yunlin 64002, Taiwan, ROC. shucm@yuntech.edu.tw

ABSTRACT

To optimize the heat transfer performance of heat exchangers, this study explored the flow properties and heat transfer of cosine-wave-shaped runners with different structural parameters (wave amplitude, focal distance, and circle radius). The effects of the changes in these structural parameters on the flow and temperature fields of specially shaped channels were analyzed. The partial synergy angles of cosine runners were obtained using user-defined programs in CFD software. The synergy of the entire channel was evaluated using the average field synergy angle as an evaluation index. This study investigated the problem of distribution nonuniformity of the temperature differences during the medium flowing process to provide a theoretical foundation and guidelines for optimally designing the structural parameters of specially shaped channels.

Introduction

Heat exchangers are indispensable to heat transfer applications. Heat exchangers provide advantages, such as convenient processing, compactness, and mature technology, and a conventional structure is generally used for their heat transfer surfaces. However, this conventional section structure leads to inevitable drawbacks, such as impeding the heat transfer to the cooling medium and sharply decreasing the condensing efficiency. Accordingly, scholars worldwide have investigated the heat transfer surfaces of specially shaped channels for heat exchangers to remedy the shortcomings observed of the conventional structure.

Manson first reported the correlation between the heat transfer and flow resistance of serrated fins; however, he used different serrated fins, which included three serrated cores and four modular experimental cores[1]. Using Kays and London's experimental data[2], Manglik and Bergles performed a simulation and confirmed the correlation between heat transfer and flow resistance[3]. Suzuki et al. and Xi et al. calculated flow characteristics in unstable regions by using two-dimensional numerical simulation[4,5]. Their results revealed apparent secondary flow phenomena and self-driving vibrations in unstable regions. Ricardo et al. researched a tubular flow channel by using three-dimensional simulation and analyzed the effects of fin pitch on heat transfer and flow properties through particle image velocimetry[6]. The investigation of trapezoidal runners began in 1931. By using the similarity solution method, Falkner et al. first derived the partial differential equations of velocity in a wedge structure[7]. Hartree and Stewartson delved into this method in more detail and found no inflection point in the velocity profile when the flow accelerated[8, 9]; however, an inflection point appeared when the flow decelerated.

Moreover, boundary layer separation appears when $\beta = -0.199\pi$. Kuo et al., Rush et al., and Rainieri and Pagliarinnihave studied numerical simulations of periodic trapezoidal structures[10–12]. In studies on fluid undergoing substantial temperature changes in the inlet section of spiral-grooved pipes, the tested Reynolds numbers have ranged from 90 to 800. On the basis of the corresponding state theory of friction coefficients, Obot et al. analyzed the critical Reynolds number of enhanced heat transfer pipes formed by cold processing smooth pipes as well as the heat transfer state under laminar and transient flow[13]. The results revealed that the lower the critical Reynolds number was, the more enhanced was the heat transfer effect.

Numerous studies have investigated the heat transfer performance of traditional heat exchangers; however, certain deficiencies and shortcomings, such as differences in the theoretical and practical structure characteristic parameters of heat exchangers, have been observed in these results. Therefore, to improve the design of heat exchangers, systematically investigating their heat transfer performance is necessary.

Physical model and structural parameters of the cosine channel

In an independent runner, a large loss of local pressure occurs when the fluid flows through a suddenly changing cross-section; however, a cosine-shaped channel provides a smooth and continuous heat transfer surface,

which alleviates resistance loss. Therefore, a half period of a cosine curve with an x-coordinate range of [0, π] was selected for the design of the heat transfer surface of a runner structure. Zhu et al., Li et al., and Zhang et al. reported that gradually expanding the structure and variation in curvature is more effective for condensate drains[14-16].

A simulation was performed to investigate the specific structural parameters of the heat transfer surfaces of cosine channels with wave amplitudes (2A = 5, 7, and 9 mm). The specific structural parameters of the heat transfer surface of the cosine channel were set as follows: S_f = 2.5 mm, h_f = 8.0 mm, and L_f = 53 mm. The working conditions were set as follows: Hot water in a tube with a constant inlet temperature and various flow rates was used to heat the air outside the tube by using the heat exchange surface and fins of specially shaped channels. Heat can be transferred from water to air. Because the air velocity at the entrance areas can be distributed uniformly, the fin length was extended by 1.5-fold in front of the entrance. To prevent the backflow phenomenon and extend the fin length by 1.5-fold at the back of the exit, the extended computational area was not repeated. (Fig. 1) presents a three-dimensional sketch of the cosine channel structure. The equation is y=Acos(Bx), where Ais determined from the height (2A) of the cosine curve and B is the runner length determined as $\lambda = 2\pi/B$, where one-half of the wavelength of the cosine curve equals the fin length ($L_f = \lambda/2$).

Mesh generation and independence analysis

As the mesh nears the wall and fin surfaces of the computational domain of the cosine channel, it becomes denser, and the calculation area became divided using structured grid partitioning. (Fig. 2a) and (Fig. 2b) illustrates the integral grid structure of an inner channel and a detailed grid structure, respectively. With structured grid partitioning, the effects of the heat transfer surface of runners with different curvatures and structures on heat transfer and resistance performance can be accurately determined. A three-dimensional model was imported into ANSYS ICEM; the model then meshed, and the mesh quality was validated to ensure that the mesh exhibited the appropriate orthogonality and aspect ratios. The boundary, initial, and other conditions were the same as those in the previous section.

In general, a moderate number of grids should be used in numerical simulations. Too many grids can result in excessive calculation times, and too few grids cannot provide sufficiently accurate results. Therefore, grid independence verification is necessary. Considering the heat exchange of a unit with 2A = 5 mm (t_f = 0.4 mm, L_f = 60 mm, h_f = 10 mm, and S_f = 4 mm), grid independence was verified when Re = 3140. Seven numbers of grids were simulated: 246,000, 400,000, 546,000, 699,000, 852,000, 997,000, and 1,101,000. The modified RNG k–ε model was adopted; the inlet velocity was u = 4 m/s, and the surface temperature of the substrate and fin was tw = 363.15 K. The simulation results revealed that both the average surface heat transfer coefficient and pressure drop of the specially shaped channel decrease with an increase in the number of grids. However, the influence of the number of grids on the computational structure weakens with > 699,000 grids. Moreover, according to the calculated results of the two models, the differences in the heat transfer coefficient and pressure drop between 997,000 and 1,101,000 grids are < 0.6%. Therefore, using 997,000 grids can satisfy requirements for convergence time, convergence accuracy, and economy.

Effects of wave amplitude on heat performance, temperature field, and flow field

(Fig. 3) demonstrates the relation between factors and f of cosine-shaped channels with three different wave amplitudes and Reynolds numbers. For each channel, L_f (53 mm), S_f (2.5 mm), and h_f (8.0 mm) are the same, but their amplitudes (2A) are different. In the graph, factors j and f decrease gradually with an increase in Re for a cosine-shaped channel with any wave amplitude. The relative increases in factors j and f primarily remain consistent as the amplitude increases and Re changes. This finding reveals that large amplitudes do not cause a

drastic change in jor f. With a decrease in the wave amplitude and the same Re, j, and f increase; that is, a small wave amplitude facilitates heat transfer but results in high friction resistance. When 2A is 5 mm, the optimal j and maximum f are obtained. Compared with the wave amplitude of 2A = 5 mm, j is 6.96% and 12.6% lower for amplitudes of 7 and 9 mm, respectively, and f is 29.8% and 50% lower, respectively.

(Fig. 3) also reveals that the maximal heat transfer factor is reached; however, the friction factor also reaches its maximum. For designing the heat transfer surface of the special-shaped channel, both friction and heat must be considered. Therefore, factor JF was used as an integrative evaluation index of heat transfer performance. Factor JF was used to compare the performance of cosine-shaped channels with three wave amplitudes (Fig. 4). The results indicated that, at the same Re, the channel with a wave amplitude of 5 mm has the best heat transfer performance.

Factor JF is expressed as follows:

$$JF = \frac{j / j_0}{\left(f_i / f_0\right)^{1/3}} \tag{1}$$

where the subscript i represents different variables (i.e., wave amplitude in the cosine-shaped channel, focal distance in the parabolic channel, or circle radius in the circular arc channel). Subscript 0 indicates the basic channel with constant sectioning. Factor JF is similar to a volume-dominant factor.

Reynolds number and amplitude effect

Effect of the Reynolds number on temperature and flow

For a deeper understanding of the heat and flow of air in the cosine-shaped channel with the different Reynolds numbers, numerical analysis was performed using the Reynolds numbers of 1210, 2170, 3140, 4110, and 5080 with a wave amplitude (2A) of 5 mm. (Fig. 5) shows the temperature programs for different Re values. The temperature of the main flow region near the middle fluid area is low, whereas that near the wall is higher, irrespective of whether the Reynolds number is small (laminar flow) or large (transitional or turbulent flow).

(Fig. 6) presents the velocity field programs for the different Re values. In this figure, red and blue respectively represent high-speed and static regions and the color range beyond red and blue represent velocities between the inlet velocity value and zero. The Reynolds numbers indicate the change from laminar to transitional and turbulent flow. The flow velocity in the main flow area near the intermediate flow area is higher, whereas near the wall surface is lower.

Effect of wave amplitudes on temperature and flow field

To study the heat transfer and flow characteristics of air in the cosine channel at different wave amplitudes with Re = 3140, channels with wave amplitudes of 5, 7, and 9 mm were numerically analyzed. (Fig. 7) illustrates the temperature field programs corresponding to different wave amplitudes. For all amplitudes, the temperature in the main flow region near the intermediate fluid region is low, and that near the wall surface is higher (Fig. 7).

(Fig. 8) delineates the velocity field programs for different wave amplitudes. The flow rate is high in the main flow region for the three-wave amplitudes because the air is affected by the viscous boundary force when flowing over the wall. Furthermore, a comparison of the three subgraphs reveals that the velocity boundary layer thickens as the wave amplitude increases. Neither backflow nor boundary layer separation occurs inside the channel, despite the increases in wave amplitude because the maximum inclination angle in the channel, corresponding to the maximum amplitude of 9 mm, has a gap creating boundary separation.

Heat transfer enhancement principle for the cosine channel

For single-phase flow, three main methods can improve heat transfer: curtailing the thickness of the thermal

boundary layer, reducing the thickness of the velocity boundary layer, and increasing the capacity of fluid perturbation through active or passive methods. Thickness reduction methods are not sufficient to provide compelling theoretical interpretations. Therefore, field synergy theory was adopted to analyze the mechanism by which heat transfer changes with the different Reynolds numbers and amplitudes. The field synergy theory integrates the heat transfer characteristics related to the aforementioned three enhancement mechanisms. The fin surface or structure could influence the field distribution characteristics, and this is mainly achieved by changing the degree of synergy between the velocity and temperature gradient vectors, which in turn changes the field synergy angle (FSA) in the whole flow field or local flow field areas. By minimizing the FSA and maximizing the integral value, the highest convection coefficient can be obtained while all other parameters of the flow field are held constant.

Therefore, the parameters were obtained to quantitatively analyze the degree of synergy between the temperature and velocity fields.

$$U \cdot \nabla T = \left|U\right| \cdot \left|gradT\right| \cos\theta \tag{2}$$

$$\theta' = \cos^{-1} \frac{u\frac{\partial T}{\partial x} + v\frac{\partial T}{\partial y} + w\frac{\partial T}{\partial z}}{\left|U\right| \cdot \left|gradT\right|} \tag{3}$$

$$\theta = \frac{\int \theta dV}{\int dV} \tag{4}$$

In these formulas, u, v, and w are the velocities of x, y, and z, respectively. U is the velocity vector, ∇T is the temperature gradient, and V is a microcontroller in a discrete fluid region.

(Fig. 9) illustrates the distribution of air in cosine channels with different wave amplitudes and the same inlet air velocity of u = 4 m/s (Re = 3140). Moreover, the position of the profile is consistent with those of the temperature and velocity field profiles. This similarity results from the cosine channel structure; therefore, different wave amplitudes do not affect this similarity. To some extent, this similarity indicates that the degree of synergy between the velocity and temperature fields in the cosine-shaped channels with three different amplitudes is similar. The same conclusion has been drawn in other experimental studies [17–19].

A simple FSA measurement cannot be used to quantitatively analyze the average angle in the overall calculation, but an average FSA could directly influence heat intensity in some aspects. Therefore, (Fig. 10) shows the curve of the average angle in the overall calculation region with different wave amplitudes. At the same Re, the average angle increases with an increase in the wave amplitude (Fig. 10).

Conclusions

In brief, three conclusions were drawn as follows:

- For a cosine channel with dimensions 5 mm ≤ 2A ≤ 9 mm, the comprehensive heat transfer performance improved with a decrease in the wave amplitude; at 2A = 5 mm, the cosine channel attained the maximal JF value.
- With the same wave amplitude, the thickness of both the thermal and velocity boundary layers decreased with an increase in Re.
- At the same Re, the average FSA gradually decreased with the wave amplitude. Therefore, a channel with a smaller wave amplitude had superior field synergy.

References

1. Manson, S.V. Correlations of heat transfer data and of friction data for interrupt plain fins staggered in successive rows. 1950, NACA Tech, Note 2237, Washington, DC, USA.
2. Kays, W.M., London, A.L. Compact Heat Exchanger. Xuan Yimin, Zhang Houlei Translate. Beijing, PR China: Science Press. 1997.
3. Manglik, R.M.; Bergles, A.E. Heat transfer and pressure drop correlations for the rectangular offset strip fin compact heat exchangers. *Exp. Thermal and Fluid Sci*. **10**, 171–180 (1995).
4. Suzuki, K., Hirai, E., Miyaki, T. Numerical and experimental studies on a two-dimensional model of an offset-strip-fin type compact heat exchanger used at low Reynold. *Int. J. Heat Mass Transfer* **28**, 823–836 (1985).
5. Xi, G., Hagiwara, Y., Suzuki, K. Flow instability and augmented heat transfer of fin arrays. *J. Enhanc. Heat Transfer*. **2**, 23–32 (1999).
6. Romero-Méndez, R., Sen, M., Yang, K.T., McClain, R. Effect of fin spacing on convection in a plate fin and tube heat exchanger. *Int. J. Heat Mass Transfer* **13**, 39–51 (2000).
7. Falkner, V.M.; Skan, S.W. Some approximate solutions of the boundary layer equations. *Phil-Mag.* **12**, 865–896 (1931).
8. Hartree, D.R. On an equation occurring in Falkner and Skan's approximate treatment of the equation of the boundary layer. *Proc. Cambr. Phil. Soc*. **33**, 223–239 (1919).
9. Stewartson, K. Further solution of the Falkner-Skan equation. Proc. Cambr. Phil. Soc **50** 454–465 (1954).
10. Kuo, J.K., Yen, T.S., Chen, C.K. Improvement of performance of gas flow channel in PEM fuel cells. *Energy Convers. Manag*. **49**, 2776–2787 (2008).
11. Rush, T.A., Newell, T.A., Jacobi, A.M. An experimental study of flow and heat transfer in sinusoidal wavy passages. *Int. J. Heat Mass Tran*. **42**, 1541–1553 (1999).
12. Rainieri, S., Pagliarini, G. Convective heat transfer to temperature dependent property fluids in the entry region of corrugated tubes. *Int. J. Heat Mass Tran*. **45**, 4525–4536 (2002).
13. Obot, N.T., Esen, E.B., Rabas, T.G. The role of transition in determining friction and heat transfer in smooth and rough passages. Int. J. Heat Mass Tran, **33** 2133–2143 (1990).
14. Zhu, D.L. Study on condensation strengthening law and structure optimization of groove vertical wall. Shanghai. *East China University of Science and Technology Engineering* **54**, 328–335 (2010).
15. Li, J., Peng, H., Ling, X. Numerical study and experimental verification of transverse direction type serrated fins and field synergy principle analysis. *Applied Thermal*. **54**, 328–335 (2013).
16. Zhang, Y., Zhang, X., Li. M., Liu, Z. Research on heat transfer enhancement and flow characteristic of heat exchange surface in cosine style runner. *Heat Mass Transf.* **55**, 3117–3131 (2019).
17. Zhang, Y.; Huang, P. Influence of mine shallow roadway on airflow temperature. Arab. J. Geosci. DOI: 10.1007/s12517–019–4934–7.
18. Zhang, Y., Li, M. Research on flow and heat transfer characteristics of heat transfer surface of trapezoidal duct. Int. J. Heat Mass Transfer DOI: 10.1007/s00231–019–02794–9.
19. Zhang, X., Zhang, Y., Liu, Z., Liu, J. Analysis of heat transfer and flow characteristics in typical cambered ducts. *Int. J. Therm. Sci*. **150**, 106-226 (2020).

Acknowledgements

This study was financially supported by the National Science Foundation of China (5187-4187, 5160-4082), the science and technology development plan project of Shandong Province (2017GSF20113), China Postdoctoral

Fund (2016M602170 and 2017T100508), Shandong Province Natural Science Foundation (ZR2018MEE002), and Beijing University of Science and Technology Ministry of Education Key Laboratory Opening Fund (ustbm-slab201802).

Author contributions statement

P. Huang put forward main research ideas. W. Huang finished the software applications. X. Lin prepared the data and the writing - first draft. C.M. Shu finished writing, commenting, and editing. All authors reviewed the manuscript.

Competing interests

The authors declare that they have no known competing financial interests or personal relationships that could have appeared to influence the work reported in this paper.

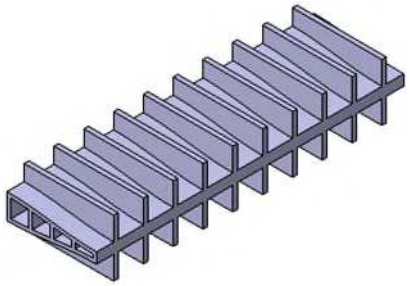

Figure 1. Three-dimension sketch graph of cosine channel.

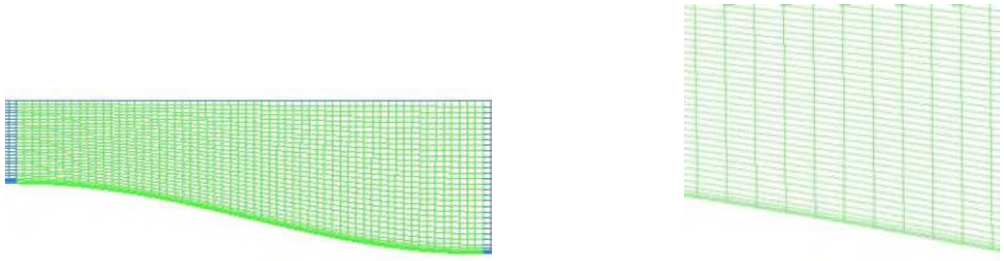

(a) Whole mesh (b) Local mesh

Figure 2. Mesh generation of cosine channel.

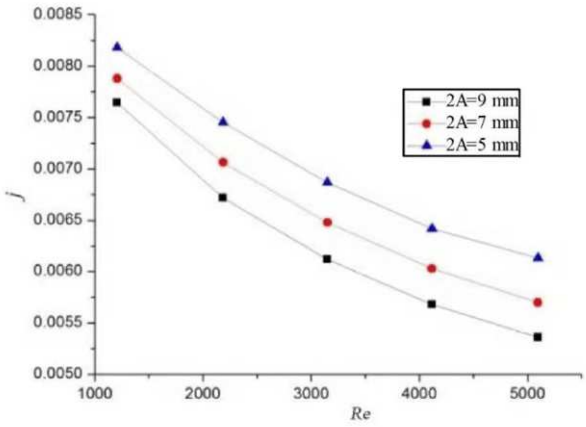

(a) j factor

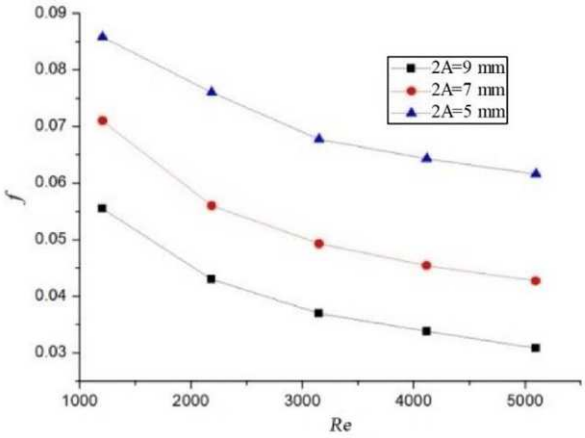

(b) f factor

Figure 3. Comparison of heat transfer and resistance properties of different wave amplitudes.

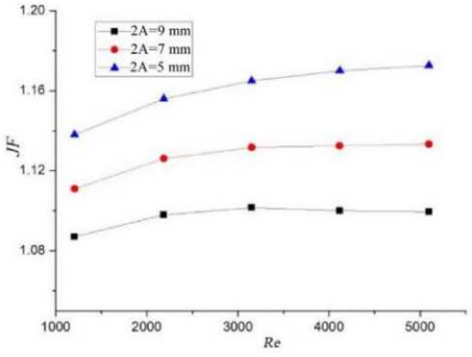

Figure 4. Comparison of enhanced heat transfer effects of three different wave amplitudes.

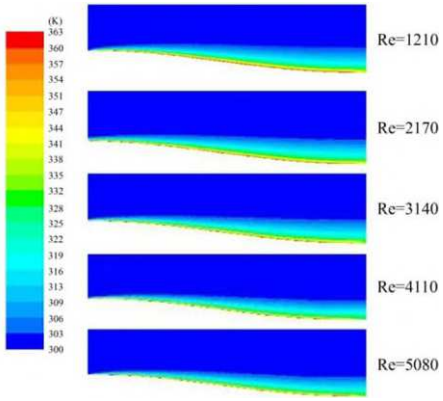

Figure 5. Influence of different *Re* (1210, 2170, 3140, 4110, and 5080) on the temperature field.

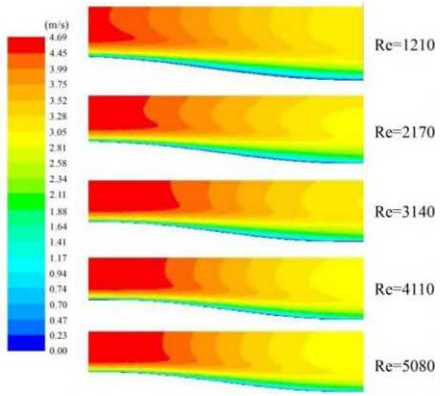

Figure 6. Influence of different *Re* (1210, 2170, 3140, 4110, and 5080) on the velocity field.

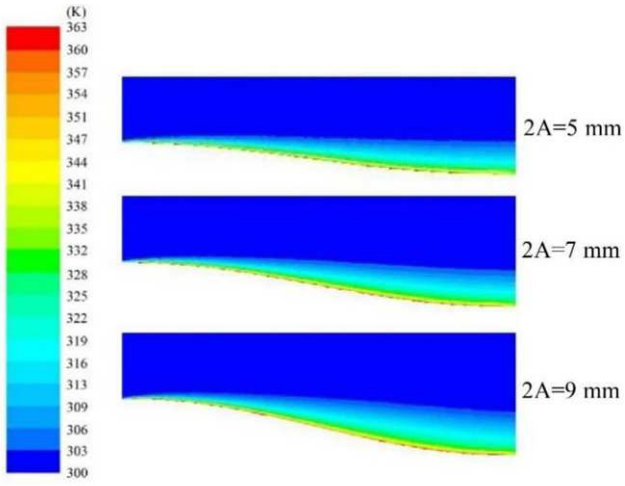

Figure 7. Influence of different wave amplitudes on the temperature field.

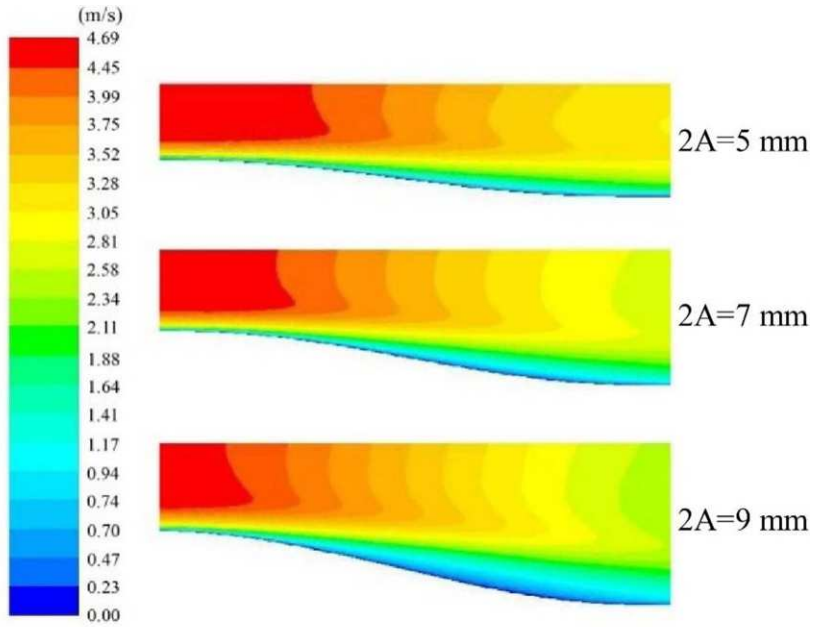

Figure 8. Influence of different wave amplitudes on the velocity field.

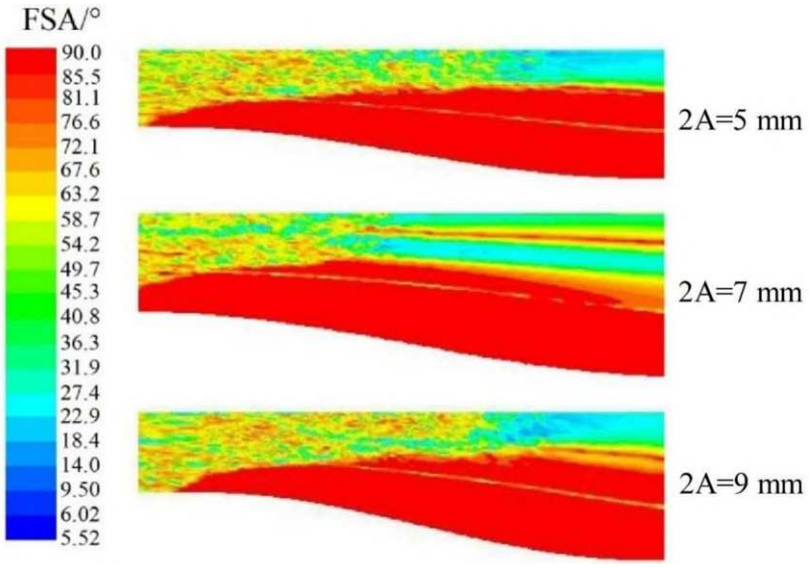

Figure 9. Local field synergy angle distribution for different 2*A* (5, 7, and 9 mm).

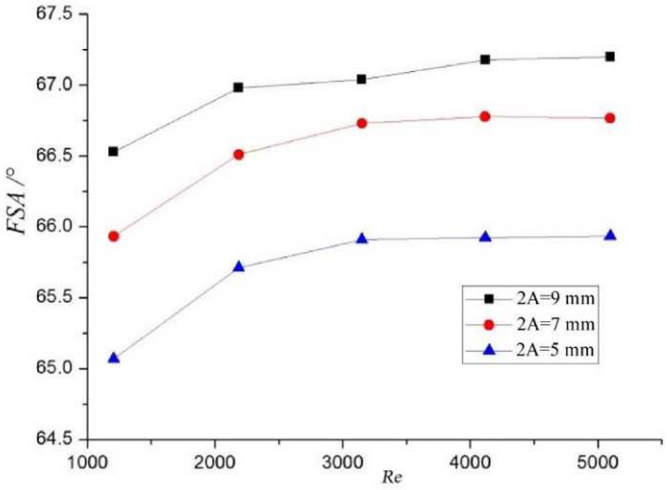

Figure 10. Comparison of average field synergy angles (FSAs) at different amplitudes.